BERKELEY ARCHAEOLOGICAL XRF LAB

Department of Anthropology

232 Kroeber Hall
University of California
Berkeley, CA 94720-3710

SOURCE PROVENANCE OF OBSIDIAN ARTIFACTS FROM MESA VERDE, SAND CANYON, DUCKFOOT, AND DOLORES PROJECT SITES, SOUTHWESTERN COLORADO

by

M. Steven Shackley, Ph.D.
Director
Archaeological XRF Laboratory
University of California, Berkeley

Celeste Henrickson, Graduate Lab Assistant

Lindsey O'Shea, Undergraduate Lab Intern

Report Prepared for

Fumi Arakawa
Department of Anthropology
Washington State University, Pullman

4 March 2005

INTRODUCTION

The analysis here of 89 artifacts from various mostly P-III period sites in southwestern Colorado is one of the largest studies of this kind in the region. Typical for sites in this region, the obsidian source provenance is dominated by sources in the Jemez Mountains, northern New Mexico, particularly El Rechuelos, Valle Grande Rhyolite, and Cerro Toledo Rhyolite obsidian. Mount Taylor obsidian in northwestern New Mexico also figures prominently. The presence of two artifacts produced from Government Mountain obsidian in two sites in this assemblage is the first time this source has been reported in southwestern Colorado to my knowledge.

LABORATORY SAMPLING, ANALYSIS AND INSTRUMENTATION

ANALYSIS AND INSTRUMENTATION

This assemblage was analyzed on a Spectrace/Thermo *QuanX* energy-dispersive x-ray spectrometer at the Archaeological XRF Laboratory, Department of Earth and Planetary Sciences at the University of California, Berkeley.

All samples were analyzed whole with little or no formal preparation. The results presented here are quantitative in that they are derived from "filtered" intensity values ratioed to the appropriate x-ray continuum regions through a least squares fitting formula rather than plotting the proportions of the net intensities in a ternary system (McCarthy and Schamber 1981; Schamber 1977). Or more essentially, these data through the analysis of international rock standards, allow for inter-instrument comparison with a predictable degree of certainty (Hampel 1984).

The spectrometer is equipped with an electronically cooled Cu x-ray target with a 125 micron Be window, an x-ray generator that operates from 4-50 kV/0.02-2.0 mA at 0.02 increments, using an IBM PC based microprocessor and WinTrace™ reduction software. The x-ray tube is operated at 30 kV, 0.14 mA, using a 0.05 mm (medium) Pd primary beam filter in an

air path at 200 seconds livetime to generate x-ray intensity Kα-line data for elements titanium (Ti), manganese (Mn), iron (as Fe^T), rubidium (Rb), strontium (Sr), yttrium (Y), zirconium (Zr), niobium (Nb), and thorium (Th). Weight percent iron ($Fe_2O_3^T$) can be derived by multiplying ppm estimates by 1.4297(10-4). Trace element intensities were converted to concentration estimates by employing a least-squares calibration line established for each element from the analysis of international rock standards certified by the National Institute of Standards and Technology (NIST), the US. Geological Survey (USGS), Canadian Centre for Mineral and Energy Technology, and the Centre de Recherches Pétrographiques et Géochimiques in France (Govindaraju 1994). Further details concerning the petrological choice of these elements in Southwest obsidians is available in Shackley (1992, 1995, 2005; also Mahood and Stimac 1991; and Hughes and Smith 1993). Specific standards used for the best fit regression calibration for elements Ti through Nb include G-2 (basalt), AGV-1 (andesite), GSP-1, SY-2 (syenite), BHVO-1 (hawaiite), STM-1 (syenite), QLO-1 (quartz latite), RGM-1 (obsidian), W-2 (diabase), BIR-1 (basalt), SDC-1 (mica schist), TLM-1 (tonalite), SCO-1 (shale), all US Geological Survey standards, JR-1 and JR-2 (rhyolite) from the Geological Survey of Japan, and BR-N (basalt) from the Centre de Recherches Pétrographiques et Géochimiques in France (Govindaraju 1994). In addition to the reported values here, Ni, Cu, Zn, and Ga were measured, but these are rarely useful in discriminating glass sources and are not generally reported.

The data from both systems were translated directly into Excel™ for Windows software for manipulation and on into SPSS™ for Windows for statistical analyses. In order to evaluate these quantitative determinations, machine data were compared to measurements of known standards during each run. Multiple analyses of RGM-1 are included in Table 1. Source nomenclature follows Baugh and Nelson (1987), Glascock et al. (1999), and Shackley (1988, 1995, 1998, 2005). Further information on the laboratory instrumentation can be found at:

http://www.swxrflab.net/ and Shackley (1998). Trace element data exhibited in Table 1 are reported in parts per million (ppm), a quantitative measure by weight (see also Figures 1 and 2).

THE JEMEZ MOUNTAINS AND VALLES CALDERA SOURCE REGION

Due to its proximity and relationship to the Rio Grande Rift System, potential uranium ore, geothermal possibilities, an active magma chamber, and a number of other geological issues, the Jemez Mountains and the Toledo and Valles Calderas particularly have been the subject of intensive structural and petrological study particularly since the 1970s (Bailey et al. 1969; Gardner et al. 1986; Heiken et al. 1986; Ross et al. 1961; Self et al. 1986; Smith et al. 1970; Figure 3 here). Half of the 1986 *Journal of Geophysical Research*, volume 91, was devoted to the then current research on the Jemez Mountains. More accessible for archaeologists, the geology of which is mainly derived from the above, is Baugh and Nelson's (1987) article on the relationship between northern New Mexico archaeological obsidian sources and procurement on the southern Plains.

Due to continuing tectonic stress along the Rio Grande, a lineament down into the mantle has produced a great amount of mafic volcanism during the last 13 million years (Self et al. 1986). Earlier eruptive events during the Tertiary more likely related to the complex interaction of the Basin and Range and Colorado Plateau provinces produced bimodal andesite-rhyolite fields, of which the Paliza Canyon (Keres Group) and probably the Polvadera Group is a part (Smith et al. 1970). While both these appear to have produced artifact quality obsidian, the nodule sizes are relatively small due to hydration and devitrification over time (see Hughes and Smith 1993; Shackley 2005). Later, during rifting along the lineament and other processes not well understood, first the Toledo Caldera (ca. 1.45 Ma) and then the Valles Caldera (1.12 Ma) collapsed causing the ring eruptive events that were dominated by crustally derived silicic volcanisim and dome formation (Self et al. 1986). The Cerro Toledo Rhyolite and Valles

Grande Member obsidians are grouped within the Tewa Group due to their similar magmatic origins. The slight difference in trace element chemistry is probably due to evolution of the magma through time from the Cerro Toledo event to the Valle Grande events (see Hildreth 1981; Mahood and Stimac 1990; Shackley 2005). This evolutionary process has recently been documented in the Mount Taylor field (Shackley 1998). Given the relatively recent events in the Tewa Group, nodule size is large and hydration and devitrification minimal, yielding the best natural glass media for tool production in the Jemez Mountains.

Recent study of the secondary depositional context of these sources and their relationship to the Rio Grande Rift have indicated that only two of the major sources enter that stream system (Shackley 2002). Cerro Toledo Rhyolite erodes from the domes in the Sierra de Toledo along the northeast scarp of the caldera, and in much greater quantity due to the ash flow tuff eruptive event associated with the Rabbit Mountain dome on the southeast margin of the caldera. This latter eruption created large quantities of glass that have continually eroded into the Rio Grande system (see Figure 3). El Rechuelos obsidian present on a number of minor domes northeast of the caldera, and slightly earlier than the caldera event, erodes north into the Rio Chama and ultimately into the Rio Grande. I find this source to be the best media for biface production of all the Jemez Mountains sources. Called “Polvadera Peak” obsidian in the vernacular, this is inaccurate since Polvadera Peak did not produce obsidian. The artifact quality obsidian is produced at smaller domes to the north of Polvadera Peak (Shackley 2005).

Obsidian from the Valle Grande member, however, does not leave the caldera floor, although some small nodules have been recovered from the East Jemez River, but does not erode outside the caldera area (Shackley 2002, 2005). This is likely due to the recent event that occurred as a resurgence on the caldera floor. Importantly, this would indicate that Valle Grande obsidian must be procured from the caldera floor proper (i.e. at Cerro del Medio) either directly

or through exchange with groups with direct access. The dominance of El Rechuelos and Valle Grande obsidian suggest selection for these raw materials. The precise social consequence of this is beyond this analysis. It is possible that it could simply be proximity, since Cerro Toledo Rhyolite obsidian erodes mainly to the southeast the direction opposite from southwestern Colorado, and thus was not as readily available to anyone arriving to the Jemez Mountains from the northwest.

A number of objects could not be assigned to known sources in western North America. This is likely due to the small sample sizes rather than an inability to assign them to a source.

REFERENCES CITED

Bailey, R.A., R.L. Smith, and C.S. Ross
1969 Stratigraphic Nomenclature of Volcanic Rocks in the Jemez Mountains, New Mexico. *U.S. Geological Survey Bulletin* 1274-P:1-19.

Baugh, T.G., and F.W. Nelson, Jr.
1987 New Mexico Obsidian Sources and Exchange on the Southern Plains. *Journal of Field Archaeology* 14:313-329.

Davis, M.K., T.L. Jackson, M.S. Shackley, T. Teague, and J.H. Hampel
1998 Factors Affecting the Energy-Dispersive X-Ray Fluorescence (EDXRF) Analysis of Archaeological Obsidian. In *Archaeological Obsidian Studies: Method and Theory*, edited by M.S. Shackley, pp. 159-180. Kluwer Academic/Plenum Press, New York and Amsterdam.

Gardner, J.N, F. Goff, S. Garcia, and R.C. Hagan
1986 Stratigraphic Relations and Lithologic Variations in the Jemez Volcanic Field, New Mexico. *Journal of Geophysical Research* 91:1763-1778.

Glascock, Michael D.
1991 *Tables for Neutron Activation Analysis* (3rd edition). The University of Missouri Research Reactor Facility.

Glascock, M.D., and M.P. Anderson
1993 Geological Reference Materials for Standardization and Quality Assurance of Instrumental Neutron Activation Analysis. *Journal of Radioanalytical and Nuclear Chemistry* 174(2):229-242.

Glascock, M.D., R. Kunselman, and D. Wolfman

1999 Intrasource Chemical Differentiation of Obsidian in the Jemez Mountains and Taos Plateau, New Mexico. *Journal of Archaeological Science* 26:861-868.

Govindaraju, K.
1994 1994 Compilation of Working Values and Sample Description for 383 Geostandards. *Geostandards Newsletter* 18 (special issue).

Hampel, Joachim H.
1984 Technical Considerations in X-ray Fluorescence Analysis of Obsidian. In *Obsidian Studies in the Great Basin*, edited by R.E. Hughes, pp. 21-25. Contributions of the University of California Archaeological Research Facility 45. Berkeley.

Heicken, G., F. Goff, J. Stix, S. Tamanyu, M. Shafiqullah, S. Garcia, and R. Hagan
1986 Intracaldera Volcanic Activity, Toledo Caldera and Embayment, Jemez Mountains, New Mexico. *Journal of Geophysical Research* 91:1799-1815.

Hildreth, W.
1981 Gradients in Silicic Magma Chambers: Implications for Lithospheric Magmatism. *Journal of Geophysical Research* 86:10153-10192.

Hughes, Richard E., and Robert L. Smith
1993 Archaeology, Geology, and Geochemistry in Obsidian Provenance Studies. *In Scale on Archaeological and Geoscientific Perspectives*, edited by J.K. Stein and A.R. Linse, pp. 79-91. Geological Society of America Special Paper 283.

Mahood, Gail A., and James A. Stimac
1990 Trace-Element Partitioning in Pantellerites and Trachytes. *Geochemica et Cosmochimica Acta* 54:2257-2276.

McCarthy, J.J., and F.H. Schamber
1981 Least-Squares Fit with Digital Filter: A Status Report. In *Energy Dispersive X-ray Spectrometry*, edited by K.F.J. Heinrich, D.E. Newbury, R.L. Myklebust, and C.E. Fiori, pp. 273-296. National Bureau of Standards Special Publication 604, Washington, D.C.

Ross, C.S., R.L. Smith, and R.A. Bailey
1961 Outline of the Geology of the Jemez Mountains, New Mexico. *Field Conference Guidebook, New Mexico Geological Society* 12:139-143.

Schamber, F.H.
1977 A Modification of the Linear Least-Squares Fitting Method which Provides Continuum Suppression. In *X-ray Fluorescence Analysis of Environmental Samples*, edited by T.G. Dzubay, pp. 241-257. Ann Arbor Science Publishers.

Self, S., F. Goff, J.N. Gardner, J.V. Wright, and W.M. Kite
1986 Explosive Rhyolitic Volcanism in the Jemez Mountains: Vent Locations, Caldera Development and Relation to Regional Structures. *Journal of Geophysical Research* 91:1779-1798.

Shackley, M. Steven
1988 Sources of Archaeological Obsidian in the Southwest: An Archaeological, Petrological, and Geochemical Study. *American Antiquity* 53(4):752-772.

1992 The Upper Gila River Gravels as an Archaeological Obsidian Source Region: Implications for Models of Exchange and Interaction. *Geoarchaeology* 7(4):315-326.

1995 Sources of Archaeological Obsidian in the Greater American Southwest: An Update and Quantitative Analysis. *American Antiquity* 60(3):531-551.

1998 Geochemical Differentiation and Prehistoric Procurement of Obsidian in the Mount Taylor Volcanic Field, Northwest New Mexico. *Journal of Archaeological Science* 25:1073-1082.

2002 Archaeological Obsidian and Secondary Depositional Effects in The Jemez Mountains and the Sierra de los Valles, Northern New Mexico. Report prepared for the Ecology Group, Los Alamos National Laboratory, New Mexico.

2005 *Obsidian: Geology and Archaeology in the North American Southwest*. University of Arizona Press, in press.

Smith, R.L., R.A. Bailey, and C.S. Ross
1970 Geologic Map of the Jemez Mountains, New Mexico. Miscellaneous Geological Investigations Map I-571. U.S. Geological Survey, Denver.

Table 1. Elemental concentrations and source assignments for the archaeological specimens.

Site/Sample	Ti	Mn	Fe	Rb	Sr	Y	Zr	Nb	Source
mt10246-134-8-29	995	452	5898	147	10	14	70	47	El Rechuelos
mt10508-39-4	1150	574	9066	193	8	62	156	83	Cerro Toledo Rhy
mt10508-63-2-39	1816	538	8845	172	6	56	148	80	Cerro Toledo Rhy
mt11338-159-2	986	483	6077	156	13	25	68	48	El Rechuelos
mt11338-196-1	1780	538	7592	149	15	13	58	41	El Rechuelos*
mt11338-213-1	1230	482	10033	165	12	35	170	44	Valle Grande Rhy
mt11338-50-2	1739	448	5753	143	16	24	57	53	El Rechuelos*
mt2149-112-1	1141	410	8315	150	9	44	157	49	Valle Grande Rhy
mt2149-113-3	1232	435	8563	144	7	47	141	52	Valle Grande Rhy
mt2149-206-1	914	566	9147	196	7	67	169	102	Cerro Toledo Rhy
mt2149-27-59	848	532	8473	186	6	59	172	99	Cerro Toledo Rhy
mt2149-27-60	918	527	8537	192	7	59	164	94	Cerro Toledo Rhy
mt2149-33-73	809	569	8645	179	8	61	167	102	Cerro Toledo Rhy
mt2149-33-74	815	392	8081	142	5	47	153	50	Valle Grande Rhy
mt2149-6-69-3500-1-1-1	1615	381	7903	138	10	34	128	35	Valle Grande Rhy
mt2149-6-69-3500-1-1-2	1697	428	7875	117	8	46	129	47	unknown
mt2149-6-69-3500-1-1-3	1265	503	9668	154	12	27	144	67	Valle Grande Rhy
mt2149-6-69-3500-1-2	953	557	8859	196	10	66	176	99	Cerro Toledo Rhy
mt2149-6-69-3500-3-1	1675	631	8643	182	5	40	127	92	Cerro Toledo Rhy
mt2149-6-69-3500-4-1	3695	349	5725	86	16	29	66	21	too small
mt2149-6-69-3500-4-2	1116	389	8004	144	5	37	157	46	Valle Grande Rhy
mt2182-15038-123	1456	414	5134	139	8	17	69	43	El Rechuelos
mt2182-15048-108	961	464	9051	162	10	47	169	58	Valle Grande Rhy
mt2182-15049-001	1854	402	5807	122	14	13	75	55	El Rechuelos*
mt2182-190-101	1186	411	5588	128	7	20	65	39	El Rechuelos
mt2182-218-001	1244	373	5224	133	10	24	70	45	El Rechuelos
mt2182-3222-206-100	1377	447	6053	145	6	16	70	51	El Rechuelos
mt2182-3311-111	1324	621	6563	166	13	24	70	48	El Rechuelos
mt2182-3384-103	886	446	5366	146	8	22	68	44	El Rechuelos
mt2182-6283-001	914	433	8229	152	11	31	159	57	Valle Grande Rhy
mt2182-6425-001	1116	449	9601	154	14	45	160	53	Valle Grande Rhy
mt2182-6489-107	1372	490	7472	97	77	16	64	59	Government Mtn*
mt2182-6500-111	2390	397	8310	121	17	38	115	34	unknown
mt2182-90003-001	1069	443	5854	115	12	14	65	52	El Rechuelos*
mt2236-82-1	2710	549	8802	170	15	51	127	69	too small
mt23-1056-001-1	986	1035	7181	488	16	76	112	164	Mount Taylor
mt23-1056-001-2	2299	547	5375	302	16	38	53	84	unknown

mt23-1056-001-3	1094	909	6790	439	7	53	88	165	Mount Taylor*
mt23-1156-003	943	426	8838	153	6	40	166	62	Valle Grande Rhy
mt23-2065-001	1771	453	5140	103	14	14	41	34	too small
mt23-2102-001	949	490	6314	159	11	17	64	61	El Rechuelos
mt23-2245-138	3429	241	5793	91	10	23	73	32	unknown
mt23-2518-001	834	552	8596	188	8	53	166	100	Cerro Toledo Rhy
mt23-298-002	1139	400	5415	132	9	20	67	52	El Rechuelos
mt23-3754-001	1463	566	6486	144	13	27	64	40	El Rechuelos
mt23-3759-104	1111	454	5910	150	13	22	59	41	El Rechuelos
mt23-4100-110	1335	556	6962	161	10	21	74	44	El Rechuelos
mt23-4294-001	1986	420	9053	145	14	38	132	47	Valle Grande Rhy
mt23-43-005	1604	433	9104	162	9	43	163	63	Valle Grande Rhy
mt23-4329-172	1105	499	5978	139	9	24	68	46	El Rechuelos
mt23-500-001	1285	450	5427	136	12	8	54	44	El Rechuelos*
Site/Sample	Ti	Mn	Fe	Rb	Sr	Y	Zr	Nb	Source
mt23-52-005	973	446	5857	152	13	19	67	55	El Rechuelos
mt23-748-002	1014	436	8376	156	13	38	157	56	Valle Grande Rhy
mt23-764-001	2390	384	7564	105	13	38	105	38	unknown
mt23-938-001	2045	417	8879	329	8	63	130	187	Mount Taylor*
mt3868-291-3	899	433	8930	152	7	37	175	54	Valle Grande Rhy
mt3868-307-3	1024	499	5762	144	14	20	62	45	El Rechuelos
mt3868-307-3	1024	499	5762	144	14	20	62	45	El Rechuelos
mt3868-329-20	829	738	8285	463	5	95	120	206	Mount Taylor
mt3868-37-11	739	723	8261	485	9	83	127	226	Mount Taylor
mt3868-415-43	1233	417	8695	152	13	36	157	60	Valle Grande Rhy
mt3868-428-20	833	685	8248	459	7	92	129	212	Mount Taylor
mt3868-66-11	773	560	7878	104	78	14	76	46	Government Mtn
mt4477-508-001	929	460	5794	139	9	21	64	48	El Rechuelos
mt4477-66-101	1673	348	7653	135	9	43	145	48	Valle Grande Rhy
mt4477-69-1	958	431	8984	155	7	42	162	52	Valle Grande Rhy
mt4477-7-100	1486	380	8074	146	6	38	157	58	Valle Grande Rhy
mt4477-83-100	1260	436	7443	193	42	18	111	26	unknown
mt4545-129-002	942	496	6427	155	11	19	71	54	El Rechuelos
mt4545-130-1	2341	537	6182	117	18	19	40	41	too small
mt4545-134-1	1511	671	7651	394	15	77	109	187	Mount Taylor*
mt4545-205-1	1500	639	8164	476	7	86	133	232	Mount Taylor
mt4545-212-1	909	394	8127	140	8	43	159	49	Valle Grande Rhy
mt4545-227-1	1810	443	5656	145	10	15	68	47	El Rechuelos
mt-4545-396-001	1017	462	8786	156	7	41	163	57	Valle Grande Rhy
mt4613-00032-001	1129	528	6453	168	9	24	65	45	El Rechuelos
mt4613-00170-100	1001	481	5820	146	10	19	68	43	El Rechuelos
mt4613-83-1	1658	478	5584	122	5	23	59	44	El Rechuelos
mt4725-207-001	856	436	5691	140	5	21	71	47	El Rechuelos
mt765-1073-18	939	455	6142	152	9	19	70	45	El Rechuelos
mt765-31-38	798	85	2701	3	20	0	10	0	not obsidian

mv1200-20913-700	2503	512	5649	97	5	10	43	39	unknown
mv1452-29247-706	1215	396	5461	140	8	22	63	46	El Rechuelos
mv1452-29967-706	1518	398	7854	144	14	36	149	48	Valle Grande Rhy
mv1452-30757-706	904	554	6285	436	6	70	100	168	Mount Taylor
mv1452-30758-706	1249	408	8140	153	10	36	152	47	Valle Grande Rhy
mv1595-32589-710	1003	538	9040	192	9	66	168	96	Cerro Toledo Rhy
mv1645-38488-711	1104	437	6028	143	7	20	67	48	El Rechuelos
mv1676-70135-1265	767	678	8327	481	10	95	131	230	Mount Taylor
RGM-1-s1	1515	297	12994	144	108	21	217	14	standard
RGM-1-s1	1573	291	12937	147	113	23	219	2	standard
RGM-1-s1	1515	297	12994	144	108	21	217	14	standard
RGM-1-s1	1498	290	13220	147	111	21	215	12	standard

* These samples are slightly outside the range of elemental concentrations, mainly due to small sample sizes (see Davis et al. 1998).

Table 2. Crosstabulation of site by obsidian source provenance.

			Source						
			El Rechuelos	Cerro Toledo Rhy	Valle Grande Rhy	Mount Taylor	Government Mtn	unknown	Total
Site/Sample	MT10246	Count	1	0	0	0	0	0	1
		% within Site/Sample	100.0%	.0%	.0%	.0%	.0%	.0%	100.0%
		% within Source	3.1%	.0%	.0%	.0%	.0%	.0%	1.2%
		% of Total	1.2%	.0%	.0%	.0%	.0%	.0%	1.2%
	MT10508	Count	0	2	0	0	0	0	2
		% within Site/Sample	.0%	100.0%	.0%	.0%	.0%	.0%	100.0%
		% within Source	.0%	20.0%	.0%	.0%	.0%	.0%	2.4%
		% of Total	.0%	2.4%	.0%	.0%	.0%	.0%	2.4%
	MT11338	Count	3	0	1	0	0	0	4
		% within Site/Sample	75.0%	.0%	25.0%	.0%	.0%	.0%	100.0%
		% within Source	9.4%	.0%	4.3%	.0%	.0%	.0%	4.8%
		% of Total	3.6%	.0%	1.2%	.0%	.0%	.0%	4.8%
	MT2149	Count	0	6	6	0	0	0	12
		% within Site/Sample	.0%	50.0%	50.0%	.0%	.0%	.0%	100.0%
		% within Source	.0%	60.0%	26.1%	.0%	.0%	.0%	14.5%
		% of Total	.0%	7.2%	7.2%	.0%	.0%	.0%	14.5%
	MT2182	Count	8	0	3	0	1	1	13
		% within Site/Sample	61.5%	.0%	23.1%	.0%	7.7%	7.7%	100.0%
		% within Source	25.0%	.0%	13.0%	.0%	50.0%	16.7%	15.7%
		% of Total	9.6%	.0%	3.6%	.0%	1.2%	1.2%	15.7%
	MT23	Count	8	1	4	3	0	3	19
		% within Site/Sample	42.1%	5.3%	21.1%	15.8%	.0%	15.8%	100.0%
		% within Source	25.0%	10.0%	17.4%	30.0%	.0%	50.0%	22.9%
		% of Total	9.6%	1.2%	4.8%	3.6%	.0%	3.6%	22.9%
	MT3868	Count	2	0	2	3	1	0	8
		% within Site/Sample	25.0%	.0%	25.0%	37.5%	12.5%	.0%	100.0%
		% within Source	6.3%	.0%	8.7%	30.0%	50.0%	.0%	9.6%
		% of Total	2.4%	.0%	2.4%	3.6%	1.2%	.0%	9.6%
	MT4477	Count	1	0	3	0	0	1	5
		% within Site/Sample	20.0%	.0%	60.0%	.0%	.0%	20.0%	100.0%
		% within Source	3.1%	.0%	13.0%	.0%	.0%	16.7%	6.0%
		% of Total	1.2%	.0%	3.6%	.0%	.0%	1.2%	6.0%
	MT4545	Count	2	0	2	2	0	0	6
		% within Site/Sample	33.3%	.0%	33.3%	33.3%	.0%	.0%	100.0%
		% within Source	6.3%	.0%	8.7%	20.0%	.0%	.0%	7.2%
		% of Total	2.4%	.0%	2.4%	2.4%	.0%	.0%	7.2%
	MT4613	Count	3	0	0	0	0	0	3
		% within Site/Sample	100.0%	.0%	.0%	.0%	.0%	.0%	100.0%
		% within Source	9.4%	.0%	.0%	.0%	.0%	.0%	3.6%
		% of Total	3.6%	.0%	.0%	.0%	.0%	.0%	3.6%
	MT4725	Count	1	0	0	0	0	0	1
		% within Site/Sample	100.0%	.0%	.0%	.0%	.0%	.0%	100.0%
		% within Source	3.1%	.0%	.0%	.0%	.0%	.0%	1.2%
		% of Total	1.2%	.0%	.0%	.0%	.0%	.0%	1.2%
	MT765	Count	1	0	0	0	0	0	1
		% within Site/Sample	100.0%	.0%	.0%	.0%	.0%	.0%	100.0%
		% within Source	3.1%	.0%	.0%	.0%	.0%	.0%	1.2%
		% of Total	1.2%	.0%	.0%	.0%	.0%	.0%	1.2%
	MV1200	Count	0	0	0	0	0	1	1
		% within Site/Sample	.0%	.0%	.0%	.0%	.0%	100.0%	100.0%
		% within Source	.0%	.0%	.0%	.0%	.0%	16.7%	1.2%
		% of Total	.0%	.0%	.0%	.0%	.0%	1.2%	1.2%
	MV1452	Count	1	0	2	1	0	0	4
		% within Site/Sample	25.0%	.0%	50.0%	25.0%	.0%	.0%	100.0%
		% within Source	3.1%	.0%	8.7%	10.0%	.0%	.0%	4.8%
		% of Total	1.2%	.0%	2.4%	1.2%	.0%	.0%	4.8%
	MV1595	Count	0	1	0	0	0	0	1
		% within Site/Sample	.0%	100.0%	.0%	.0%	.0%	.0%	100.0%
		% within Source	.0%	10.0%	.0%	.0%	.0%	.0%	1.2%
		% of Total	.0%	1.2%	.0%	.0%	.0%	.0%	1.2%
	MV1645	Count	1	0	0	0	0	0	1
		% within Site/Sample	100.0%	.0%	.0%	.0%	.0%	.0%	100.0%
		% within Source	3.1%	.0%	.0%	.0%	.0%	.0%	1.2%
		% of Total	1.2%	.0%	.0%	.0%	.0%	.0%	1.2%
	MV1676	Count	0	0	0	1	0	0	1
		% within Site/Sample	.0%	.0%	.0%	100.0%	.0%	.0%	100.0%
		% within Source	.0%	.0%	.0%	10.0%	.0%	.0%	1.2%
		% of Total	.0%	.0%	.0%	1.2%	.0%	.0%	1.2%
Total		Count	32	10	23	10	2	6	83
		% within Site/Sample	38.6%	12.0%	27.7%	12.0%	2.4%	7.2%	100.0%
		% within Source	100.0%	100.0%	100.0%	100.0%	100.0%	100.0%	100.0%
		% of Total	38.6%	12.0%	27.7%	12.0%	2.4%	7.2%	100.0%

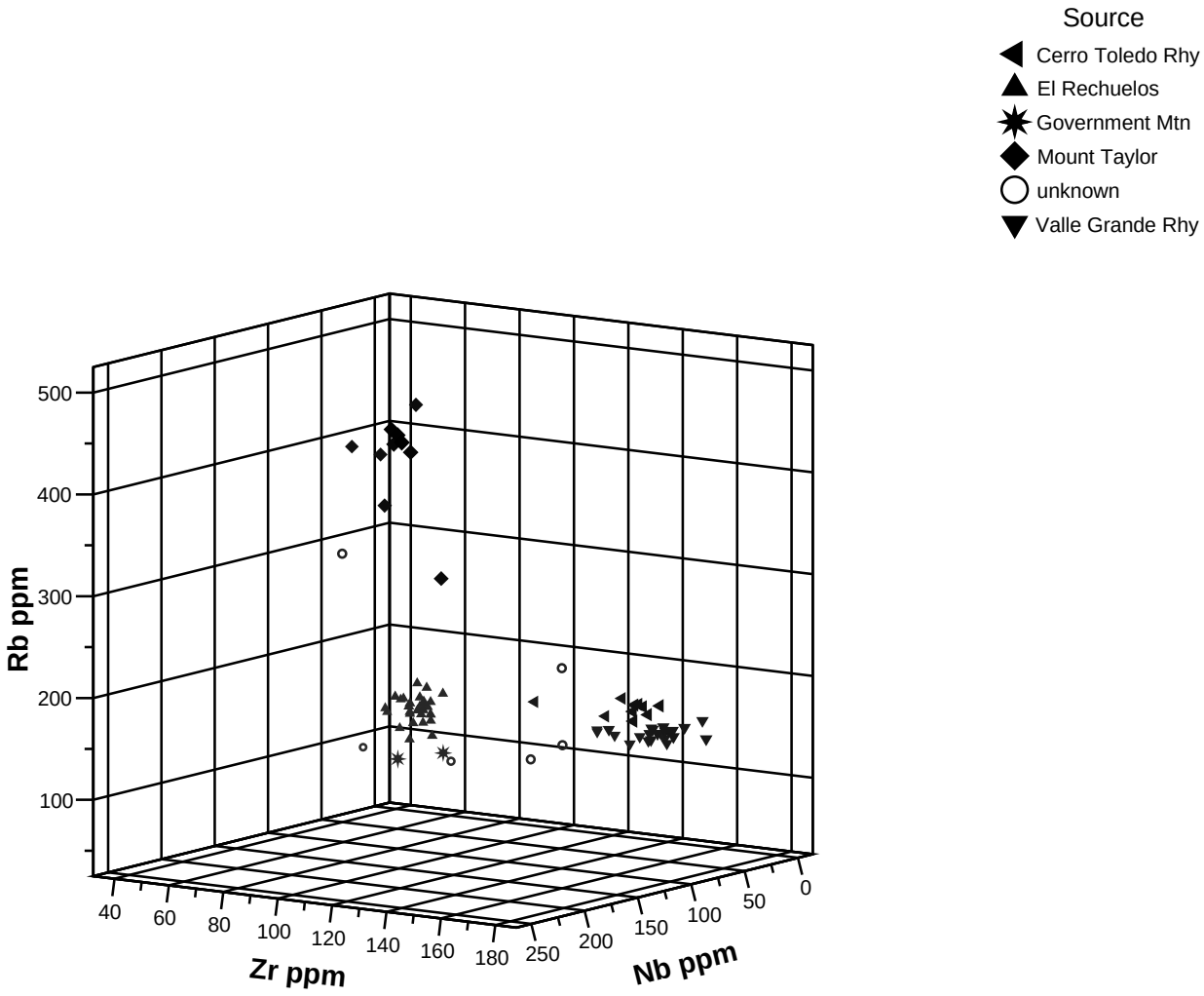

Figure 1. Rb, Zr, Nb three-dimensional plot of the elemental concentrations for the archaeological specimens.

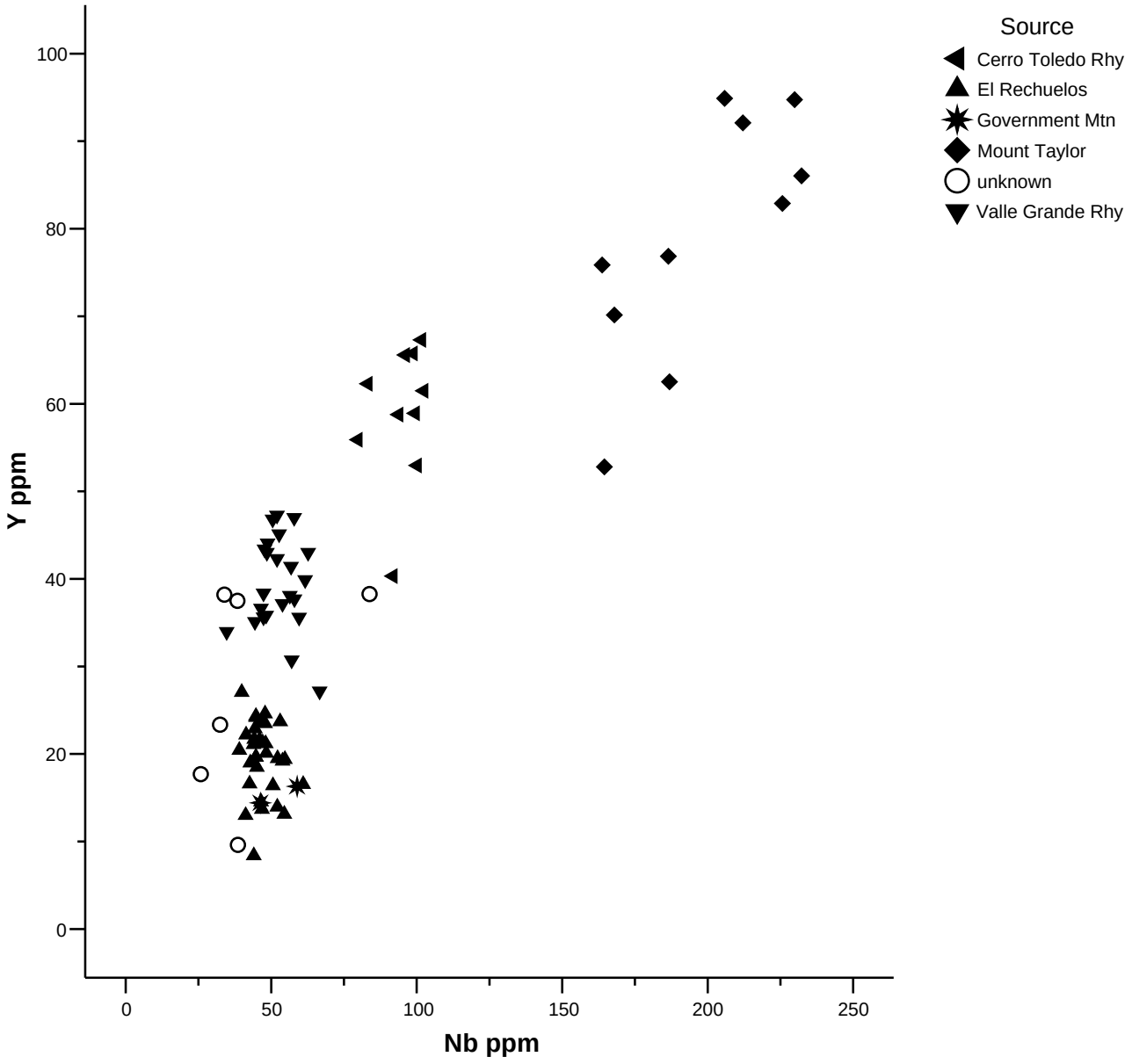

Figure 2. Y versus Nb biplot of archaeological specimens more effectively separating the Jemez Mountains sources. Note the the "unknowns" and Goverment Mountain are not grouped with the Jemez Mountains sources in the three-dimensional plot.

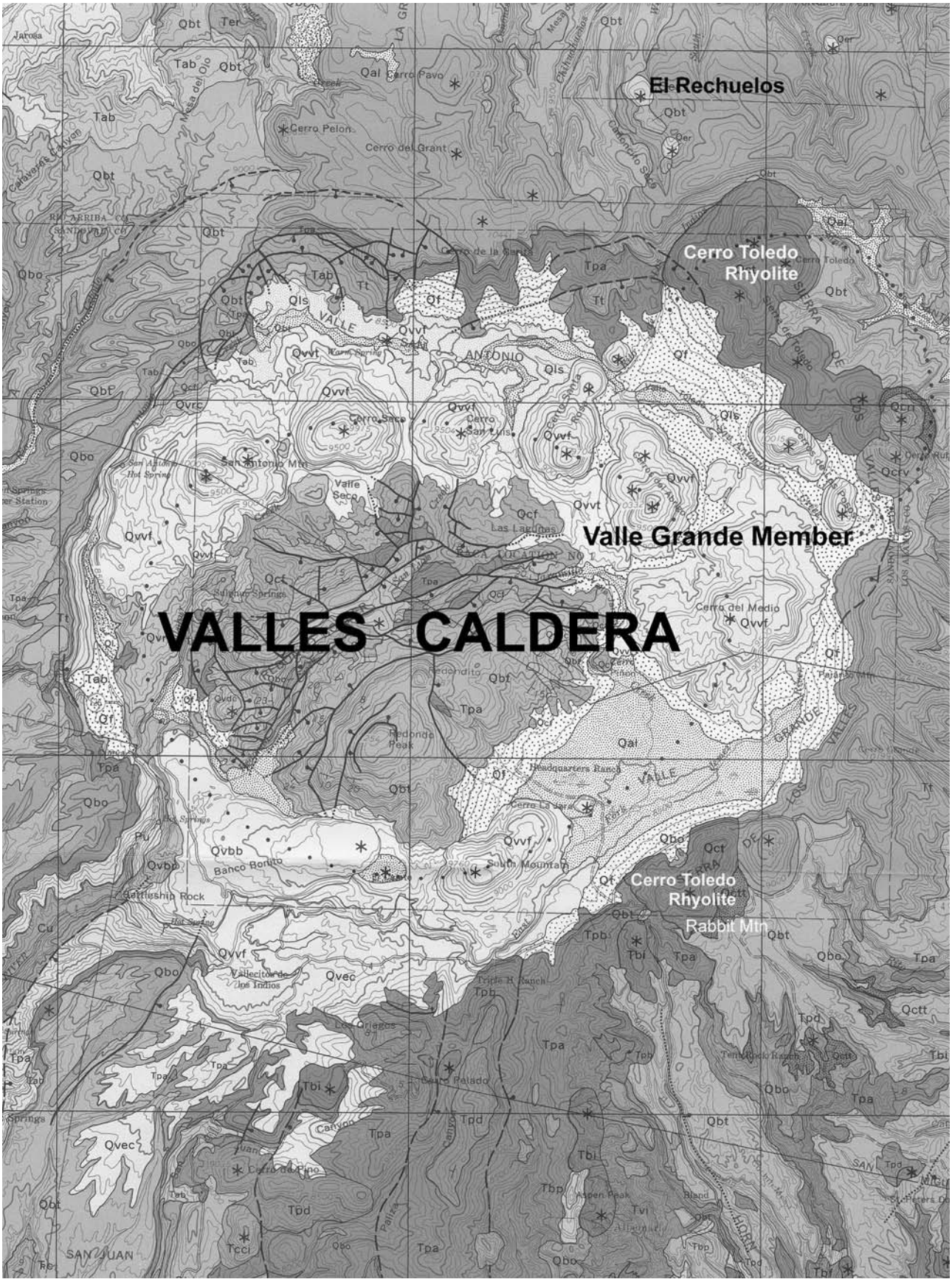

Figure 3. Topographical rendering of a portion of the Jemez Mountains, Valles Caldera, and relevant features. (from Baugh and Nelson 1987; Smith et al. 1970).